ELSEVIER

Physica B 294–295 (2001) 319–323

PHYSICA B

www.elsevier.com/locate/physb

Magnetotransport in mesoscopic carbon networks

V.A. Samuilov[a,d,*], J. Galibert[b], V.K. Ksenevich[c,d], V.J. Goldman[e], M. Rafailovich[a], J. Sokolov[a], I.A. Bashmakov[d], V.A. Dorosinets[d]

[a]*Department of Materials Sciences, SUNYSB, Stony Brook, NY 11794-2275, USA*
[b]*Laboratoire National des Champs Magnétiques Pulsés, 143, Avenue de Rangueil, F-31432 Toulouse, CEDEX 4, France*
[c]*Johann Wolfgang Goethe-University, Robert-Mayer-Str. 2-4, D-60054 Frankfurt/Main, Germany*
[d]*State University of Belarus, 220080 Minsk, Belarus*
[e]*Department Physics, SUNYSB, Stony Brook, NY 11794-3800, USA*

Abstract

The temperature and magnetic field dependencies of the resistance of regular carbon mesoscopic networks were studied in a temperature range from 4.2 to 300 K and in pulsed magnetic fields up to 35 T. A crossover from Mott variable range hopping to the Coulomb-gap Efros–Shklovskii regime has been observed. From the magnetoresistance versus magnetic field curves three regions were defined of low, intermediate and high magnetic field. At low fields, $\ln(R/R_0)$ is proportional to B^2. In the intermediate range, the magnetoresistance is linear with B. The dependence of magnetoresistance on B in the high-field region is much weaker. At high temperatures, where the hopping distance is low enough to be compared with the localization length, we observe small negative magnetoresistance in our samples.

Keywords: Mesoscopic carbon networks; Strong localization; Magnetoresistance; High magnetic fields

1. Introduction

The mesoscopic and nano-scale periodic structures have attracted considerable attention recently from scientific and technical point of view [1–3]. This interest originates from various novel characteristics, such as photonic band gap [4,5]. As far as electrical properties, 2-D mesoscopic periodic structures have provided many experimental results on the metallic side of the metal–insulator transition [6–10]. By contrast, there have been very few experimental studies of electrical transport phenomena in mesoscopic periodic structures for the strongly localized electrons [11,12]. So far, it is not clear, if their characteristic dimensions, like the size of the cell and the thickness of bonds are effective for transport properties.

The mesoscopic and nano-scale periodic structures with electrical transport through strongly localized states may be produced by relatively simple methods either of infiltration of the regular arrays of uniform silica particles [5,12] or by mesoscopic patterning in polymer solutions in the presence of humid atmosphere [13,14]. The insulating polymers are carbonized by heat treatment in vacuum [15]. The structural and electrical properties can be controlled by the temperature of heat

* Correspondence address. Tel.: + 631-632-4736; fax: + 631-632-5764.
E-mail addresses: vsamuilov@notes.cc.sunysb.edu (V.A. Samuilov).

0921-4526/01/$ - see front matter
PII: S0921-4526(00)00668-2

treatment. Various structures from disordered glass-like to graphite carbon materials were obtained [16,17]. In this paper, we give the results of resistance and magnetoresistance (MR) measurements of regular mesoscopic carbon networks.

2. Experimental details

A simple approach of nonlithographic fabrication of two-dimensional periodic mesoscopic networks with the feature size (the thickness of the bonds) down to 50 nm and the size of the cells of order of 500 nm has been developed. The technique is based on the self-organized patterning in a thin layer of complex liquid-diluted nitrocellulose solution in the presence of humid atmosphere. The sub-micron sized water droplets were trapped at the surface and form compact regular aggregates. The polymer was found to precipitate at the water–polymer solution interface, forming a layer encapsulating the droplets and preventing their coalescence. After the evaporation of the solvent the networks were transferred onto insulating substrates. The final carbon structures (Fig. 1) were produced by heat treatment of the nitrocellulose precursors at relatively low temperatures $T = 750$–1500°C.

Regular 4-point probe contacts in van-der-Pauw and linear geometry were produced on top of the carbon networks. Magnetoresistance measurements were carried out in pulsed magnetic fields, at the Laboratoire National des Champs Magnétiques Pulsés de Toulouse (LNCMP), in the temperature range 1.6–300 K, and up to 35 T.

Here we present the typical results on the group of samples heat treated in vacuum at $T = 950^{\circ}$C for 1 h. The results of the influence of heat treatment on electrical transport properties of carbon mesoscopic networks will be discussed later.

3. Zero-field resistance

We assume that the data of the dependence of the resistance on temperature can be fitted by the general expression for variable range hopping (VRH)

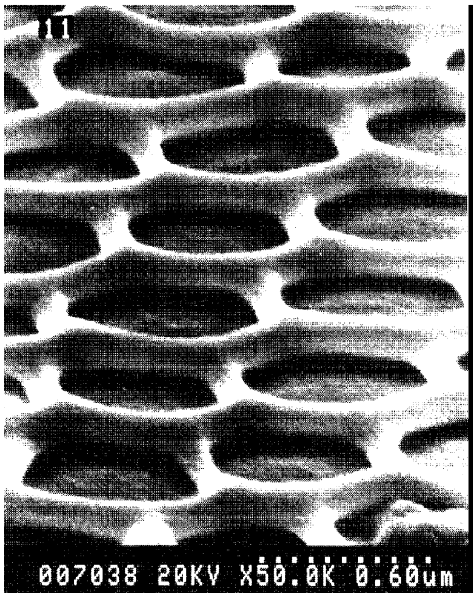

Fig. 1. The scanning electron microscopy image of the carbon mesoscopic network.

transport [18]:

$$R = R_0 \exp[(T_0/T)^s]. \quad (1)$$

Expecting a crossover from Mott (M) ($s = \frac{1}{4}$) to Efros–Shklovski (E–S) ($s = \frac{1}{2}$) when the temperature decreases and the system becomes 'more insulating', we plot the zero-field resistance $R_s(T, B = 0)$ as a function of $T^{-1/2}$ and $T^{-1/4}$ [19] in the Fig. 2. We can easily see two temperature regions with different behaviour of the resistance. The R_s versus T data were analyzed using a procedure suggested by Zabrodski [20] just to determine an approximate value of the crossover temperature T_c at the interception of the linear fitting curves for two different temperature regions. The value obtained was $T_c \approx 13$ K. The temperature range was divided into two regions: 4.24–11.96 K and 14.4–301 K for treatment of Efros–Shklovskii and Mott VRH mechanisms, respectively. Using a nonlinear fitting procedure by minimizing the least-squares deviation $\chi^2 = \Sigma[\ln(R_{exp}) - \ln(R_{calc})]^2$ [21], the best exponent values for each temperature range were found to be 0.508 ± 0.032 and 0.306 ± 0.015. Both values are relatively close to 0.5 and 0.25, respectively. For these fixed exponent values the charac-

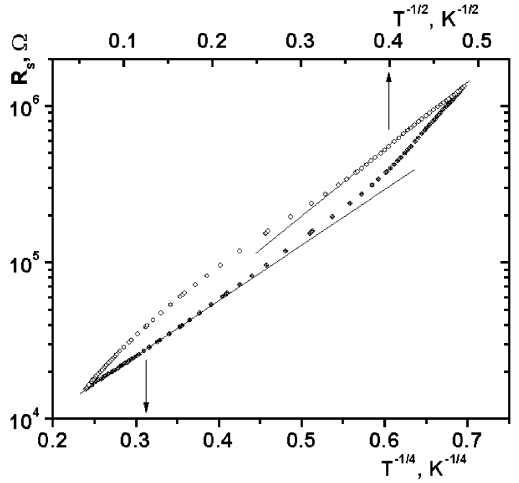

Fig. 2. The temperature dependence of the resistance as a function of $T^{-1/2}$ (upper axis) and as a function of $T^{-1/4}$ (lower axis) at zero magnetic field.

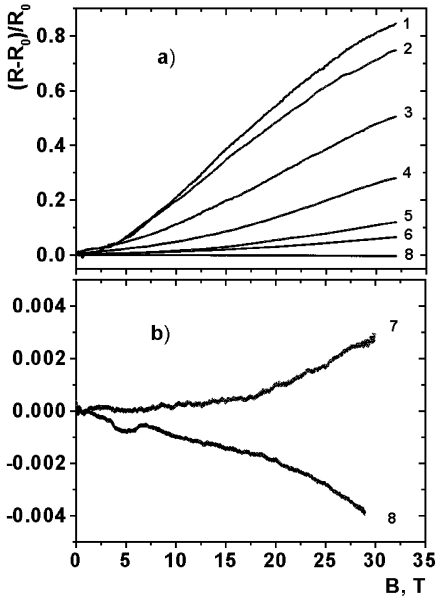

Fig. 3. The magnetoresistance as a function of magnetic field at different temperatures T: 1–4.2 K, 2–5.15 K, 3–8.98 K, 4–11.44 K, 5–17.03 K, 6–25.0 K, 7–50.0 K, 8–99.7 K.

teristic temperatures were determined: $T_{ES} = 104.9\,K$ and $T_M = 5008\,K$. Let us note that 2-D VRH conduction mechanism with $s = \frac{1}{3}$ could be considered also in the framework of these data.

The relation between T_c, T_{ES} and T_M is the following [20–22]:

$$T_C = \alpha T_{ES}^2 / T_M. \quad (2)$$

The dimensionless parameter $\alpha = 16$ for the case of the equality of the hopping energies in the two regimes when the crossover occurs [20]. If different criterion to determine the crossover temperature is used: at T_C the width of the 'optimal band' ΔT of localized levels which are involved in the hopping conduction becomes equal to the half-width of the Coulomb gap, $\alpha = 2.7$ [21]. For our experimentally determined values of $T_{ES} = 104.9\,K$ and $T_M = 5008\,K$ the calculated value of $\alpha = 5.9$, which is reasonable.

4. Magnetoresistance

In Fig. 3(a) and (b) we show the MR data. From the MR versus B curves (Fig. 3(a)), three regions were defined of low, intermediate and high magnetic field. At low fields, $\ln(R - R_0/R_0)$ is proportional to B^2. In the intermediate range, the MR is nearly linear with B. The MR dependence on B in the high-field region is much weaker and tends to saturation at the highest fields and the lowest temperatures. The field range of these regions is very sensitive to temperature and decreases with temperature. At 4.2 K we observed the B^2 dependence up to $B \sim 8.2\,T$. While at 11.4 K it is seen up to $B \sim 14.1\,T$. The intermediate range also gets narrower with decreasing temperature. At high temperatures ($T > 50\,K$) the small (less than 0.5%) negative MR was observed (Fig. 4b).

It was reported [23], that in carbon-black polymer composites a large positive MR at low temperatures and a small negative MR at higher temperatures had been observed. As soon as the hopping distance R_h is related to the localization length ξ [24]: $R_h \sim \xi\sqrt{T_{ES}/T}$, at higher temperatures they may be comparable, and we observed small negative MR, which could be consistent with the weak-localization picture [25], for example.

In the E–S regime the relative MR is given by [18]:

$$R(T,B)/R(T,0) = \exp[K_s(T)B^2], \quad (3)$$

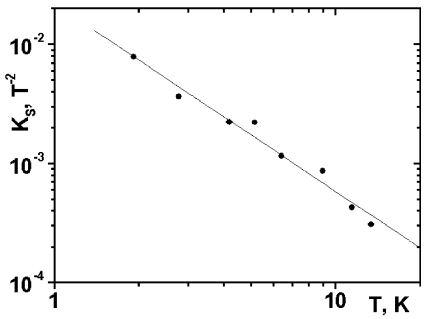

Fig. 4. The coefficient K_s obtained from the dependence $\ln[R(B)/R(0)] = K_s B^2$ in the low-field regimes vs. temperature T on a log–log plot.

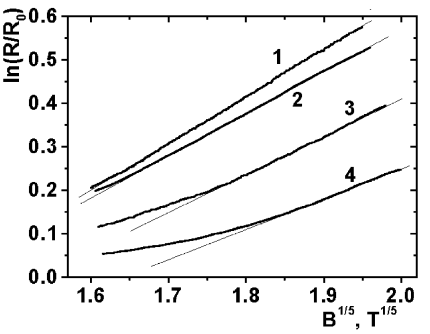

Fig. 5. The plot of $\ln(R(B)/R_0)$ as a function of $B^{1/5}$ in the high magnetic field range at different temperatures within the ES regime: 1–4.2 K, 2–5.15 K, 3–8.98 K, 4–11.44 K.

where in the E–S VRH regime K_s depends on the temperature [18,22]:

$$K_s = \frac{e^2\xi^4}{C_1\hbar^2}\left[\frac{T_{ES}}{T}\right]^{3/2}, \tag{4}$$

where e is the electron charge, C_1 the dimensionless constant of the order of 10^3 [24] ($C_1 = 660$ [26]), $\hbar$ the Plank constant. For an experimental determination of K_s we plotted the low-field MR versus B^2 for different fixed temperatures (not shown). A plot of the temperature dependence of the slope K_s obtained from linear dependence $\ln[R(B)/R(0)] = K_s B^2$ for each temperature, in the low-field regimes is shown in Fig. 4. The determined experimental value of the slope $\log K_s$ versus $\log T$ is $K_s = -1.58 \pm 0.10$, which is in close agreement with the theoretical coefficient of the low-field E–S VRH regime, i.e. close to -1.5.

From the analysis of the low-field data, we can calculate the value of the localization length (Eq. (5)), employing the zero-field value of T_{ES}. We found the localization length to be $\xi = 8.75$ nm. The density of states in the vicinity of E_F in SE regime [18]

$$g_{CG}(E) = g_0|E - E_F|^2, \tag{5}$$

where the characteristic factor of the Coulomb gap

$$g_0 = \frac{3(\varepsilon\varepsilon_0)^3}{\pi e^6}, \tag{6}$$

with $\varepsilon\varepsilon_0$ being the dielectric constant.

As far as the characteristic hopping temperatures T_{ES} is related directly to the localization length by the expression [18]:

$$T_{ES} = \frac{\beta_1 e^2}{\varepsilon\varepsilon_0\xi}, \tag{7}$$

where the dimensionless parameter $\beta_1 = 2.8$, we can determine g_0, combining Eqs. (6) and (7). We found $g_0 = 2.7 \times 10^{13}\,\mathrm{cm}^{-3}\,\mathrm{K}^{-3}$. Note, that this method of deducing of the factor g_0 assumes that the values T_{ES} and ξ are not changed too much with respect to the magnetic field [22].

In the high field regime, where the Coulomb gap is important, the magnetic field dependence of the resistance is expected to vary as [18]

$$R(T,B) = R_0 \exp\left(\frac{T_0(B)}{T}\right)^{3/5}, \tag{8}$$

where $T_0 \propto B^{1/3}$.

In the Fig. 5, we plotted $\ln(R(B)/R_0)$ as a function of $B^{1/5}$, as it follows from Eq. (8) at different temperatures. We can see the linearity in these plots at high magnetic fields. The range of the dependence of the Eq. (8) is wider at lower temperatures.

5. Conclusions

The crossover from Mott variable range hopping to the Coulomb-gap Efros–Shklovskii mechanism upon decreasing of temperature has been

experimentally observed in regular mesoscopic carbon networks.

At low magnetic fields, $\ln(R - R_0/R_0)$ is proportional to B^2. The dependence of MR on B in the high-field region is much weaker: $\ln(R(B)/R_0) \propto B^{1/5}$. At high temperatures ($T > 50$ K) we observed small negative MR.

Acknowledgements

This work was supported in part by the Foundation of Basic Research of Belarus under Grant No. F99-319, NSF-MRSEC Program and the NSF under Grant No. DMR 9986688.

One of us (V.S.) would like to acknowledge the financial support from the French Ministry of Education through a C.I.E.S fellowship and a hospitality of Laboratoire National des Champs Magnétiques Pulsés de Toulouse.

V.K. acknowledges DAAD for financial support and Prof. H. Roskos for hospitality.

References

[1] S.H. Park et al., Adv. Mater. 10 (1998) 1045.
[2] A.A. Zakhidov et al., Science 282 (1998) 897.
[3] S.A. Jonson et al., Science 283 (1998) 963.
[4] J.D. Joannopoulos et al., Nature 386 (1997) 143.
[5] K. Yoshino et al., Jpn. J. Appl. Phys. 36 (1997) L714.
[6] B. Pannetier et al., J. Phys. 44 (1983) L853.
[7] B. Pannetier et al., Phys. Rev. Lett. 53 (1984) 718.
[8] B. Pannetier et al., Phys. Rev. B 31 (1985) 3208.
[9] G.J. Dolan et al., Phys. Rev. Lett. 56 (1986) 1493.
[10] M.E. Gershenson et al., Phys. Rev. Lett. 56 (1986) 1493.
[11] Ya.B. Poyarkov et al., JETP Lett. 44 (1986) 372.
[12] K. Yoshino et al., Jpn. J. Appl. Phys. 38 (1999) 4926.
[13] N. Maruyama et al., Thin Solid Films 327–329 (1998) 854.
[14] O. Pitos et al., Eur. Phys. J. B 8 (1999) 225.
[15] T. Takeichi et al., Carbon 37 (1999) 569.
[16] H. Ueno et al., Phys. Rev. B 34 (1986) 7158.
[17] Y. Hishiyama et al., Carbon 31 (1993) 1265.
[18] B.I. Shklovskii, A.L. Efros, Electronic Properties of Doped Semiconductors, Springer Series of Solid State Science, Springer, Berlin, 1984.
[19] A.G. Zabrodski et al., JEPT 59 (1984) 425.
[20] R. Rosenbaum, Phys. Rev. B 44 (1991) 3599.
[21] I. Shlimak et al., Phys. Rev. Lett. 68 (1992) 3076.
[22] M. Iqbal et al., Phil. Mag. B 79 (1999) 1591.
[23] P. Mandal et al., Phys. Rev. B 55 (1997) 452.
[24] A.W.P. Fung, Phys. Rev. B 49 (1994) 17325.
[25] E. Medina, Phys. Rev. B 46 (1992) 9984.
[26] A.G. Zabrodski, Sov. Phys. Semicond. 14 (1980) 670.